New techniques to sound the composition of the lower stratosphere and troposphere from space

B.J. Kerridge, R. Siddans, J. Reburn, V. Jay and B. Latter

CCLRC, Rutherford Appleton Laboratory,
Chilton, Oxfordshire, OX11 0QX
b.j.kerridge@rl.ac.uk

ABSTRACT

This paper outlines three new techniques to sound the composition of the lower stratosphere and troposphere from space which are under development by the RAL Remote Sensing Group within NERC's Data Assimilation Research Centre. The focus is on retrieval of ozone, water vapour and other trace gases whose distributions are directly or indirectly important to climate. The first technique is to combine information from Hartley band absorption with temperature-dependent differential absorption in the Huggins bands to retrieve height-resolved ozone profiles spanning the troposphere and stratosphere from observations of backscattered solar uv radiation by ESA's Global Ozone Monitoring Experiment (GOME). To illustrate the performance of the RAL scheme, ozone distributions and linear diagnostics are presented along with comparisons with ozonesondes and other space observations. The second technique is to exploit the synergy between limb- and nadir- observations of a given airmass to retrieve profiles spanning the troposphere and stratosphere which improve on those attainable by either geometry individually. Results are presented from the first application of this technique in the retrieval domain to co-located measurements from Envisat MIPAS and ERS-2 GOME. The third technique is to retrieve horizontal as well as vertical structure (ie 2-D fields) in the upper troposphere and lower stratosphere through tomographic limb-sounding. This is illustrated with linear diagnostics and constituent fields retrieved by the RAL scheme in non-linear, iterative simulations for (a) a mm-wave limb-sounder (MASTER) and (b) Envisat MIPAS in its UTLS Special Mode (S6). Finally, the current status and plans for future work in these areas are summarised.

1 Background

The distributions of certain trace gases in the troposphere and stratosphere can influence climate either directly (eg H_2O and O_3) through their radiative properties or indirectly (eg tropospheric CO or stratospheric ClO) through chemical interactions with radiatively active gases. The tropospheric distributions of trace gases such as O_3, CO and CH_4 reflect surface emission fluxes as well as chemical and physical processes occurring within the atmosphere. Tracer distributions can supplement the information on dynamics which can be derived from temperature fields. For these and other reasons, considerable attention is now being paid to the assimilation by global models of satellite observations of H_2O, O_3 and other trace gases.

The aim of the RAL Remote-Sensing Group within the NERC Data Assimilation Research Centre is to produce novel global data-sets for assimilation by applying new techniques to sound the composition of the lower stratosphere and troposphere from space. In the following sections of this paper, three such techniques are briefly described.

2 Ozone Profiles from GOME

A scheme has been developed to retrieve height-resolved ozone profiles from measurements of solar uv backscattered radiation made by ESA's Global Ozone Monitoring Experiment (GOME) on ERS-2. A novel feature of the RAL scheme is to exploit temperature dependent differential absorption structure in the Huggins' bands to extend to lower altitudes the information on stratospheric ozone which can be retrieved from the Hartley band. The strong, wavelength-dependent opacity of ozone in the Hartley band (260-310nm) has long been exploited by NASA's "BUV" type instruments and offers useful, height-resolved information down to the altitude of peak ozone concentration. In the RAL scheme, this is used as *a priori* information for a second step employing the Huggins bands. Two pre-requisites for this are: (1) contiguous spectral coverage at $\approx$0.2nm sampling afforded by GOME (cf measurements in discrete spectral bands of $\approx$1nm width by the "BUV" type instruments) and (2) fitting precision in the 325-335nm interval of $<$0.1% RMS (cf 1% in the Hartley band). To achieve a fitting precision of $<$0.1% RMS, a number of instrumental and geophysical variables additional to ozone must be accounted for. The value of adding the Huggins bands is illustrated in 1 which compares averaging kernels for the Hartley band only with those for the combined Hartley and Huggins bands for a retrieval level spacing of 6km and an *a priori* uncertainty of 100% at all levels. Averaging kernels for the Hartley band are seen to have well-defined peaks only in the stratosphere, whereas those for the composite retrieval are seen to be well-behaved also in the troposphere. An independent intercomparison of averaging kernels has recently been performed by BIRA-IASB for the ESA Working Group on GOME Ozone Profile Retrieval (V.Soebijanta, pri.comm.). Figures 2 and 3 present the six most significant eigenvectors of the averaging kernel matrices for a typical ozone profile retrieval by the RAL scheme and by the IFE and KNMI schemes. The 5th and 6th eigenvectors of the RAL matrix are seen to have significant contributions from the lower troposphere, unlike the other two schemes.

Profiles retrieved by the RAL scheme have been validated against a large ensemble of ozonesondes and also concurrent satellite observations. A number of sub-sets of data have been processed from the period 1995-9 (www.badc.rl.ac.uk) and a seasonal climatology of height-resolved ozone which spans the troposphere as well as the stratosphere has recently been produced [Siddans (2003)]. Figure 4 displays seasonal mean maps of ozone retrieved in the lower troposphere from ground-pixels in which cloud fraction has been estimated to be $<$0.05 Elevated ozone concentrations over south-east Asia and central America during northern hemisphere spring are associated with biomass burning. Over the USA, the north Atlantic and Europe, ozone concentrations are highest in summer because of photochemical production from primary pollutants and the prevailing westerlies. Anomalously high concentrations near the coast of Antarctica in southern spring are retrieval artifacts associated with ozone hole occurrence in the overlying stratosphere which are under investigation. Absence of data in a region extending over much of South America and the neigbouring Atlantic is because detector dark-current fluctuations caused by particle impact in the South Atlantic Anomaly prevent the use of the Hartley band.

From 1999 onwards, degradation of the GOME scan-mirror surface has caused a serious reduction in its uv reflectivity. This reduction in reflectivity has been found to depend strongly on time, wavelength and view angle and exhibits the properties of a Fabry-Perot etalon of steadily increasing thickness. Because this reduction is greater in the direct-sun view than in the nadir-view, sun-normalised radiances actually appear to have increased (by up to 80%) after 1998. An empirical correction scheme has been devised by fitting a 2-D Legendre polynomial, of 4th order in wavelength and 14th order in time, to the fractional difference between sun-normalised spectra between 260 and 310nm measured by GOME and predicted by a radiative transfer model using the Fortuin and Kelder climatology [Fortuin and Kelder (1998)] (figure 5). An initial assessment through comparisons with ozonesondes in 1998 and summer 2002 (figure 6) indicates that the correction scheme is functioning adequately. The standard deviation of retrieved profiles with respect to the sondes is comparable or even smaller in 2002. The bias is also comparable in 2002, except in the 12-16km

layer where it has increased from ≈+10% to ≈+20%.

The RAL scheme has a negative bias of several 10's% in the 0-6km layer. Simulations have shown that inadequate knowledge of slit-function shape in the Huggins bands can give rise to a bias of this magnitude [Kerridge et al. (2002),Siddans (2003)].

The impact of the degradation correction on data quality in the stratosphere has also been gauged through an assimilation exercise (M.Juckes, pri.comm.). Figure 6 shows scatter plots of assimilated GOME data vs MIPAS, SAGE-III, HALOE and GOME itself on the 650K potential temperature surface (≈30hPa) for September 2002. The assimilated GOME data are biased with respect to the SAGE-III and HALOE solar occultation observations by +0.24 and +0.55ppmv, respectively, ie <10%[1].

Initial indications from comparisons with ozonesondes and other satellite instruments are therefore that the degradation correction is performing sufficiently well to justify processing data from 1999-2003 as well as 1995-1998, ie the full (8-year) mission, to examine interannual variability in the troposphere and stratosphere.

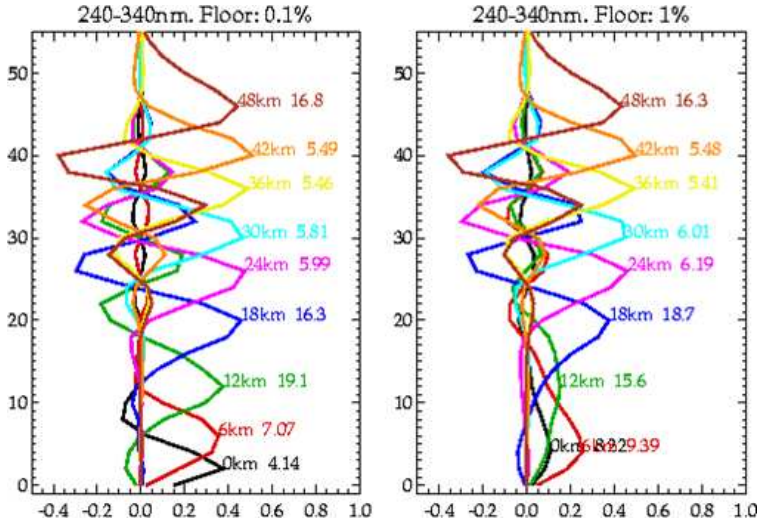

Figure 1: Composite averaging kernels for an O_3 retrieval from GOME Bands 1 and 2 adopting, for clarity, a uniform retrieval level spacing of 6km and an a priori *uncertainty of 100% at each level. In the right-hand panel, a noise floor of 1% has been imposed, which is appropriate for Band 1 (Hartley band) but effectively excludes information from Band 2 (Huggins bands). In the left hand panel, a noise floor of 0.1% is imposed, which is appropriate for Band 2, showing the benefit in the troposphere of adding the Huggins bands.*

[1]MIPAS data exhibited anomalous variability, especially at high southern latitudes, in the version used here, which has been reduced in subsequent versions

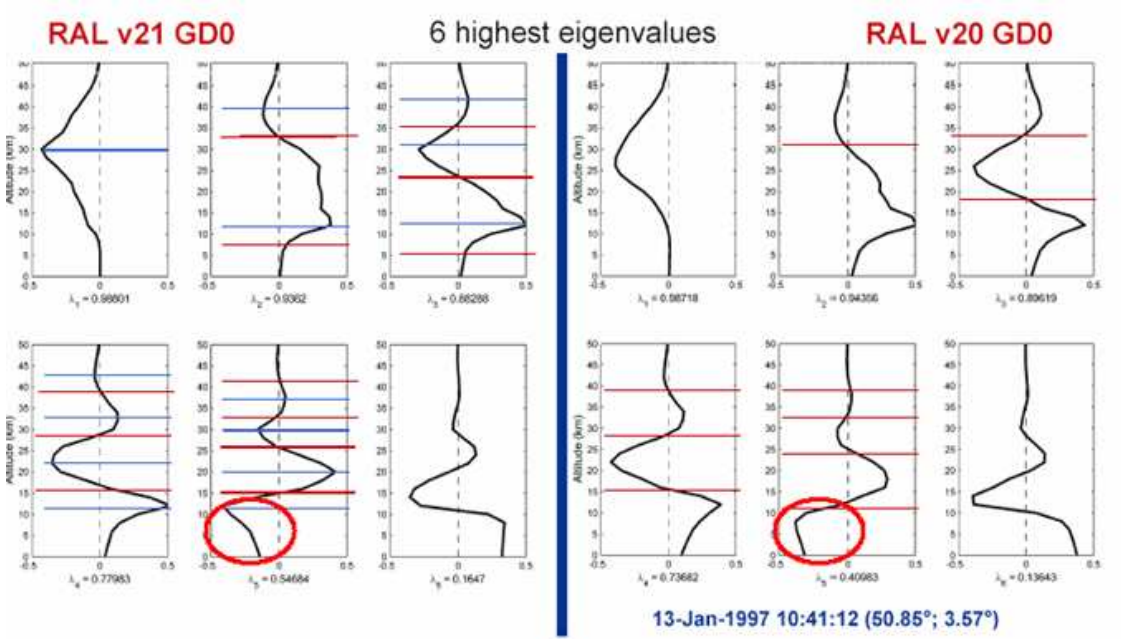

Figure 2: The six most prominent eigenvectors of the averaging kernel matrix for a typical O_3 retrieval (13th Jan 1997 at 10:41:12; 50.85N 3.85E) by the RAL scheme, as calculated by V.Soebijanta (BIRA-IASB) for the ESA GOME O_3 Profile Working Group. In the right panel, the standard ESA L1 data have been used and in the left panel additional calibration corrections have been applied to the L1 data by KNMI.

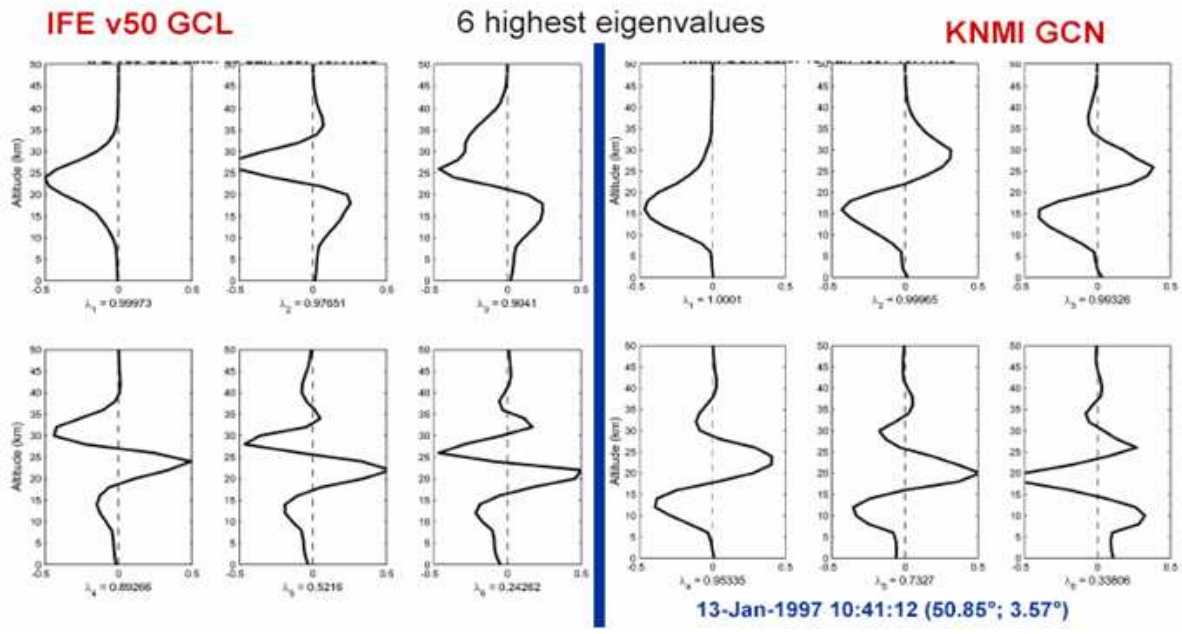

Figure 3: The six most prominent eigenvectors of the IFE and KNMI averaging kernel matrices for O_3 retrievals from the same ground pixel as figure 2

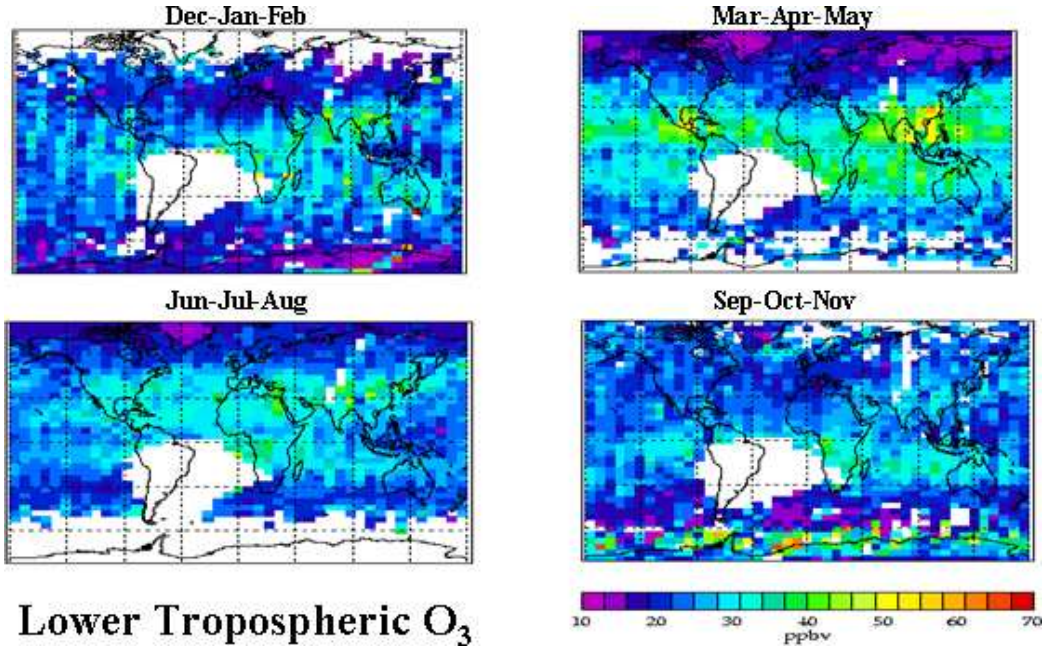

Figure 4: Seasonal mean distributions of O_3 in the lower troposphere derived from sub-sets of GOME data processed by the RAL scheme in the four year period 1995-8. Values are presented for the surface retrieval level although, due to vertical smearing, they actually represent an average over the lower troposphere. Data have been screened to include only ground-pixels for which cloud fraction is estimated to be <0.05.

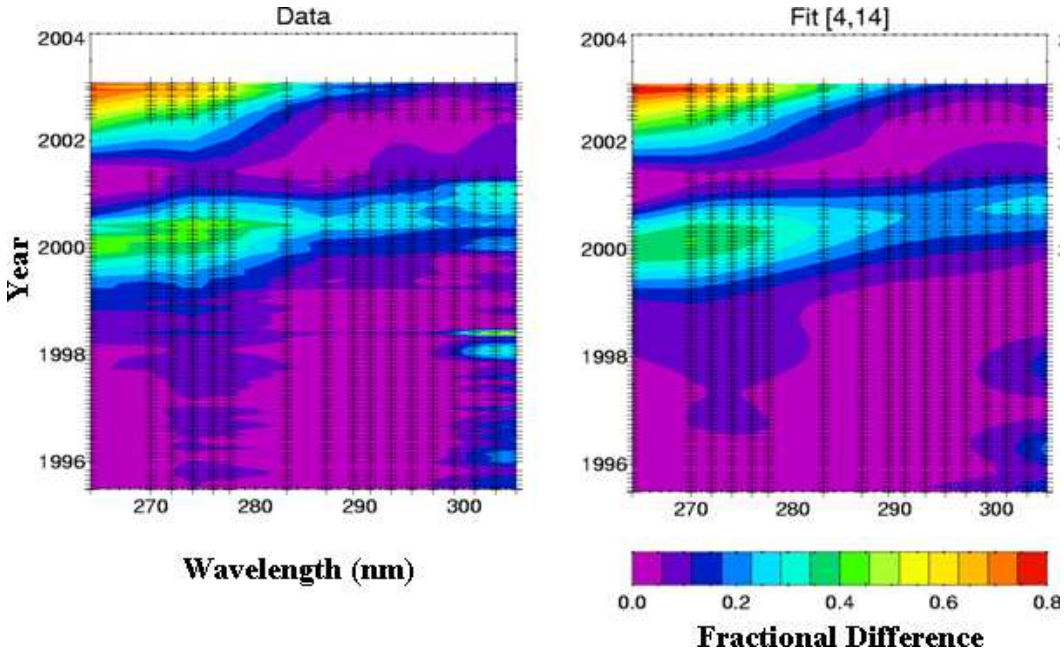

Figure 5: Fractional deviation between the sun-normalised radiance spectrum (260-310nm) measured by GOME and that predicted by a radiative transfer model based on the Kelder and Fortuin O_3 climatology, plotted as a function of time. The left hand panel shows the average deviation for one day per month over the period 1995 - 2003, sampling every fifth Band 1 ground pixel on a given day within the latitude range 65S to 80N. The right panel shows a 2-D Legendre polynomial fit to these deviations, of 4th order in wavelength and 14th order in time.

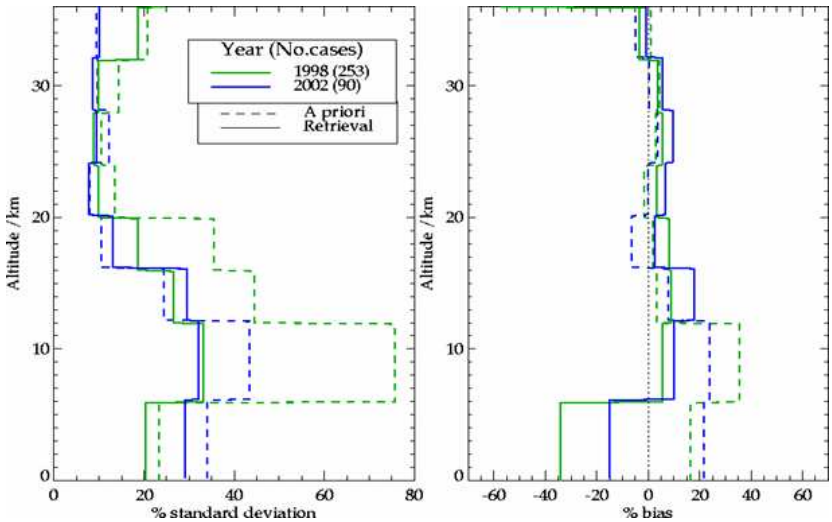

Figure 6: Comparison of O_3 profiles retrieved by the RAL scheme in cloud-free ground pixels with co-located ozonesondes, before (1998) and after (2002) the onset of scan-mirror uv degradation. The left panel shows the standard deviation of layer-averaged fractional differences between a priori *and retrieved O_3, on one hand, and the corresponding ozonesonde profile, on the other. It should be noted that northern hemisphere winter and spring were sampled in 1998 but not in 2002 so, in the latter case, the standard deviation of* a priori *with respect to ozonesondes is very much lower. The right panel shows the mean of the layer-averaged fractional differences, indicative of the biases of* a priori *and retrieved O_3 with respect to the ozonesondes. Retrieval bias in the 0-6km layer is likely to be due to error in the slit-function shape used in modelling the Huggins bands.*

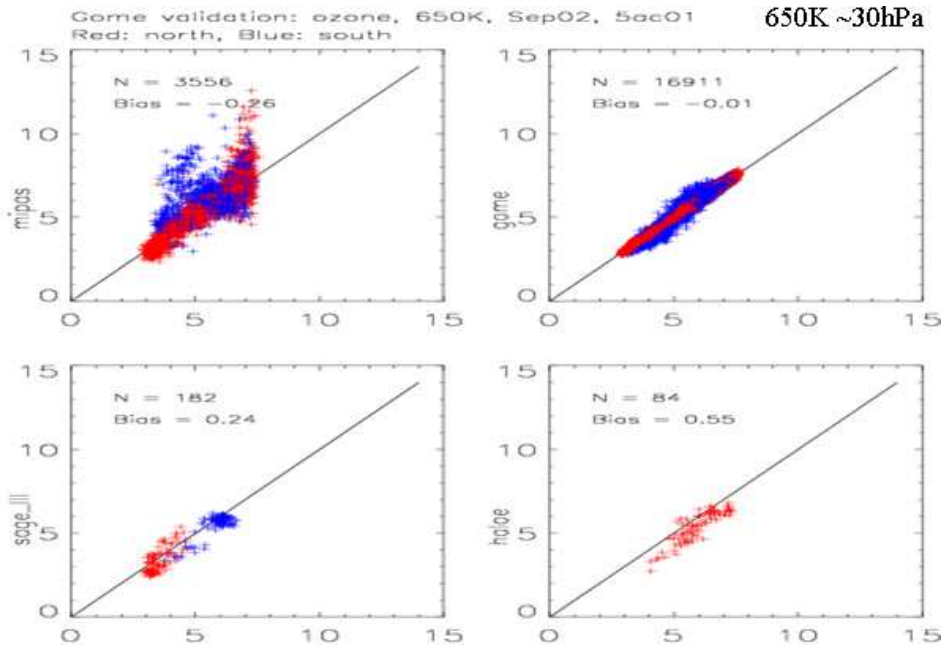

Figure 7: Comparison of assimilated GOME O_3 data produced by the RAL scheme in September 2002 with concurrent observations by HALOE, SAGE-III and MIPAS (M.Juckes, pri.comm.). The four panels show scatter plots output from an assimilation of GOME height-resolved O_3 data on the 650K potential temperature surface (near 30hPa) at locations of observations by the other three sensors along with GOME itself. The top right panel shows the assimilated O_3 data to be unbiassed with respect to the input GOME O_3 values.

3 Limb-nadir synergy

It is well known that the characteristics of limb- and nadir-viewing geometries are complementary. In the absence of cloud, nadir-sounders can see to the Earth's surface[2]. However, their vertical resolution is controlled by atmospheric radiative transfer properties and is comparatively low (>4km with the exception of tropospheric H_2O). Limb-sounders, by contrast, rarely see to the Earth's surface but their vertical resolution and sensitivity are both high due to, respectively, discrete sampling in the vertical and longer optical paths. It has been recognised [Langen and Fuchs (2001),Kerridge et al. (2001)] that a future space mission to sound atmospheric composition should exploit the complementary characteristics of limb- and nadir-viewing as fully as possible.

Limb-sounding has traditionally been used to observe the stratosphere and mesosphere (eg UARS, Odin). However, recent advances in millimetre-wave technology and the development of tomographic techniques (see next section) enable the current generation of satellite limb-sounders (eg ESA Envisat and NASA Aura) to penetrate also into the troposphere. In principle, by characterising accurately a constituent's distribution in the stratosphere and upper troposphere, limb-sounding observations should also permit its lower tropospheric distribution to be retrieved more accurately than from nadir-sounding observations alone. This is especially so for a constituent whose concentration is larger in the stratosphere and/or upper troposphere, of which ozone is a prime example.

The potential benefit to ozone of limb-nadir synergy has been demonstrated in the data assimilation frame by combining stratospheric profile information from UARS MLS with total column information from GOME [Struthers et al. (2002)]. A significant first step has now been made towards limb-nadir synergy in the retrieval domain by using MIPAS operational L2 products as a strong *a priori* constraint for GOME ozone profile retrieval from the Huggins bands only. The MIPAS L2 profiles therefore substitute for those retrieved from the Hartley band in the first step of the standard GOME retrieval (section 2). A necessary pre-requisite for this exercise was the level of agreement (within $\pm$10% throughout the stratosphere) which had been found previously between MIPAS operational L2 products and the standard RAL GOME retrieval scheme (with degradation correction applied).

Although the MIPAS L2 profiles extend below the tropopause, contamination from cloud at these lower altitudes had not been flagged in the version available for this experiment. The ozone climatology which is normally used as *a priori* for the RAL GOME scheme was therefore overwritten only in the stratosphere. The *a priori* field combining MIPAS information in the stratosphere with climatological information in the troposphere can be compared with its two components in figure 8. The ozone field retrieved from the GOME Huggins bands with a strong stratospheric constraint from MIPAS may be compared in figure 8 with that retrieved from the GOME Hartley and Huggins bands constrained by the standard ozone climatology. Deviations of the combined GOME(Huggins)/MIPAS retrieval and of the standard GOME retrieval with respect to the MIPAS L2 field are also shown. The combined retrieval overcomes the most obvious limitations of the individual sensors, namely: absence of a GOME Hartley band retrieval in the SAA region (see section 2) and cloud contamination of MIPAS observations below the tropopause. While following closely the structure of the MIPAS stratospheric field, structure captured in the troposphere is similar to the standard GOME retrieval and therefore constitutes a satisfactory first demonstration of limb-nadir synergy in the retrieval domain.

[2]It should be noted that trace gas detection at IR wavelengths depends upon temperature contrast with the surface, so sensitivity is very low in the boundary layer.

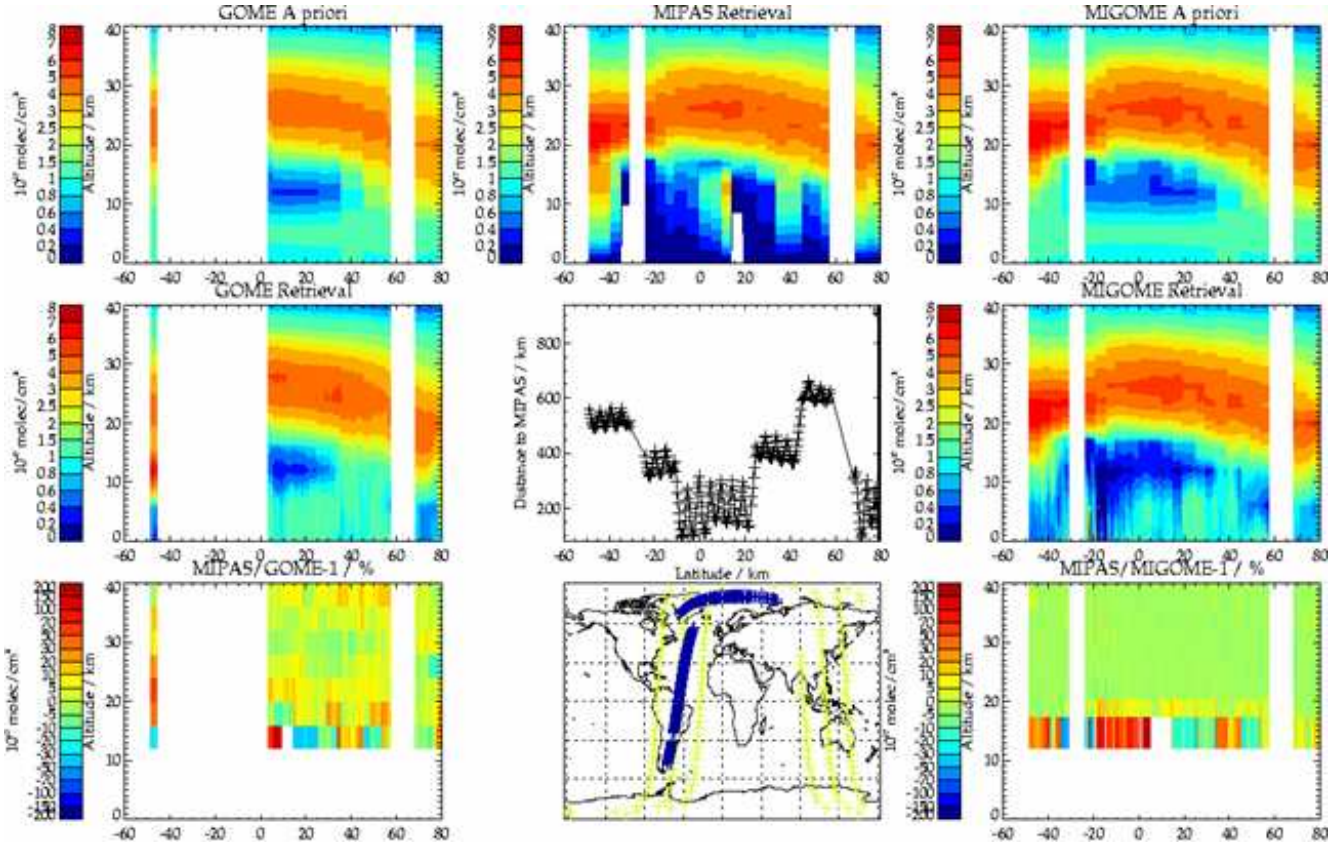

Figure 8: First demonstration of limb/nadir synergy in the retrieval domain by combining Envisat MIPAS and ERS-2 GOME. Envisat and ERS-2 follow the same orbit tracks, although MIPAS scans in azimuth towards the poles at high latitudes, so its tangent-point track deviates from the orbit track. The GOME orbit track and three closest MIPAS tangent-point tracks are shown in the bottom centre panel, and the horizontal displacement between each GOME observation and the closest MIPAS limb-scan are shown in the panel above. The standard a priori *distribution for the GOME O_3 retrieval is shown in the top left panel and the output from the combined Hartley and Huggins bands retrieval is shown in the panel below, with data missing in the south Atlantic anomaly (SAA). ESA's MIPAS O_3 L2 data at locations closest to GOME are shown in the top centre panel, with cloud contamination evident in the upper troposphere, most notably at 12km near 10N. The top right panel shows an* a priori *distribution which merges MIPAS L2 data in the stratosphere with the standard GOME* a priori *in the troposphere. The centre right panel shows output from a GOME Huggins band only retrieval which has been tightly constrained to the MIPAS L2* a priori *in the stratosphere. Desirable features of the synergistic retrieval in comparison to the standard GOME retrieval and the MIPAS L2 data are, respectively, coverage in the SAA and absence of cloud contamination in the upper troposphere. The bottom left and bottom right panels show fractional differences between MIPAS L2 data and the standard GOME retrieval and the synergistic retrieval, respectively.*

4 Tomographic limb-sounding

To invert limb-sounding observations, it is usual to: (a) adopt a model of the atmosphere which comprises a series of concentric shells within which physical properties and composition vary only with altitude and (b) retrieve a single vertical profile from a given limb-scan. In reality, the lowest stratosphere and troposphere are characterised by horizontal as well as vertical variability, so profiles retrieved in the conventional manner are, at best, an average over the true field and, at worst, compromised by inconsistencies between observed and modelled radiances. The tomographic limb-sounding technique is intended to alleviate these limitations of conventional limb-sounding. The assumption of spherical symmetry is dropped in favour of a 2-D atmosphere in the radiative transfer model; the state vector comprises atmospheric fields on a 2-D grid rather than a 1-D profile and the measurement vector comprises a set of limb-scans which are inverted simultaneously. Provided that the atmospheric limb is scanned in the vertical plane of the satellite orbit vector and the spacing between adjacent tangent-points is fine enough to oversample that of the state vector, a given air volume will be viewed from a number of different directions, conferring a tomographic advantage.

The principles of tomographic limb-sounding are straightforward and the CPU speed and addressable memory of computers now make feasible the practical implementation of this technique. However, certain simplifications are still required to make the computational problem tractable. A tomographic retrieval scheme is under development at RAL for application to mm-wave and IR limb-emission observations which solves the iterative (ie non-linear) Optimal Estimation equation.

$$x_{i+1} = x_i + (S_a^{-1} + K_i^T S_y^{-1} K_i)^{-1} (K_i^T S_y^{-1} (y - F(x_i)) + S_a^{-1} (x_a - x_i)) \quad (1)$$

A simplification adopted in this scheme is to accumulate the matrix $K_i^T S_y^{-1} K_i$ sequentially, on a limb-view by limb-view basis. This requires the S_y matrix to be diagonal, ie measurement errors to be uncorrelated from one limb-view to the next. This permits the dimension of arrays to be stored to be reduced from N_y (which would be unfeasibly large) to N_x. Since N_x is itself large, further matrix manipulation is still required to make the computational problem viable.

The RAL 2-D scheme has now been applied in extensive simulations for the proposed ESA mm-wave limb-sounder (MASTER). Linear diagnostics have been examined to: assess retrieval precision, vertical and horizontal resolution; to gauge sensitivity to various errors and to specify instrument requirements. Iterative simulations have also been performed in the presence of realistic errors to assess the accuracy with which 2-D structure in UTLS fields of H_2O, O_3, CO and other species could potentially be retrieved. The use of linear diagnostics is illustrated in figure 9, which plots H_2O retrieval precision vs horizontal grid spacing at different altitudes. These simulations assume an antenna half-power beamwidth of ≈2.3km, vertical and horizontal tangent-point spacings of 1km and 64km, respectively, and 2km vertical spacing in the retrieval grid. *A priori* uncertainty is 100no correlations. Useful precision (10's %) is seen to be attainable in the upper troposphere for horizontal spacings in the retrieval grid down to <100km, which is much finer than the horizontal resolution traditionally associated with limb-sounding (≈500 - 1000km).

Iterative (cloud-free) simulations have been conducted for a number of 2-D scenarios using temperature, H_2O and O_3 fields from ECMWF analyses and 2-D distributions of other trace gases constructed with an equivalent potential vorticity approach [Lary (1995)]. In figure 10, 2-D cross-sections retrieved from MASTER measurements are compared to the true cross-sections used to synthesise these. The *a priori* and initial guess fields for these retrieval simulations had no horizontal gradients, yet much of the structure in the true fields is captured quite well. The obvious exception is the altitude range in which limb-paths are opaque, which is controlled by tropospheric H_2O, and therefore varies with geographical location and frequency band. The retrieval scheme generally performs well up to H_2O mixing ratios of ≈400ppmv.

An iterative (cloud-free) simulation has also been conducted (M.Parrington, pri.comm.) using the RAL scheme for O_3 retrieval from the Envisat MIPAS UTLS special mode (S6). The S6 mode has been designed to permit the tomographic technique to be demonstrated for the first time; sampling in the standard MIPAS mode is too sparse for this. Sampling patterns for the standard and S6 modes are shown in figure 11. The S6 mode has narrower vertical spacing between limb-views in the UTLS (2km cf 3km) and much narrower along-track spacing (112km cf 512km). To compensate, it scans only up to 30km tangent-height (cf 68km) and its spectral sampling is lower by a factor 4 (0.1cm^{-1} cf 0.025cm^{-1}).

By comparison to 10, it is apparent that O_3 can be retrieved to lower altitudes by MIPAS in cloud free scenes, although the extinction efficiency of cirrus is known to be much higher at IR than mm wavelengths. In a current ESA study, it is planned to perform 2-D simulations for mm-wave and IR limb-sounders which incorporate clouds and also to devise a climatology of the occurrence of clouds which impact significantly on mm-wave and IR limb-sounding. This is intended to provide a more realistic evaluation of their respective capabilities in the upper troposphere.

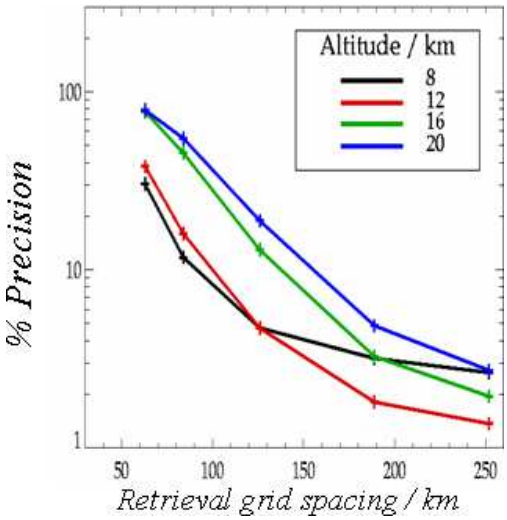

Figure 9: Trade-off between H_2O retrieval precision at different retrieval altitudes and retrieval grid horizontal spacing. The curves show how precision (S_x diagonal) varies with horizontal grid spacing in a 2-D simulation for MASTER, as all other parameters are held constant (see text).

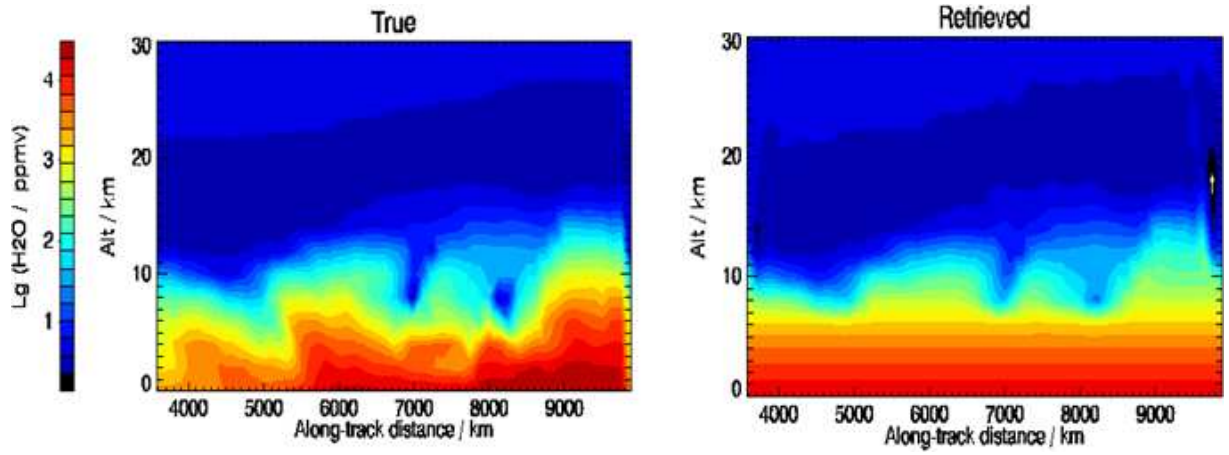

Figure 10: Iterative simulation of a 2-D H_2O cross-section retrieval from the MASTER 325 GHz band. The left panel shows an H_2O cross-section (30km vertical × 6,000km horizontal) extracted from an ECMWF analysis field. The right panel shows output from a 2-D iterative retrieval for MASTER 325GHz band measurements synthesised from this field and the corresponding temperature field, with noise and other realistic errors (temperature and pointing) added. Structure in the true field is seen to be captured down to the altitude at which limb-paths become opaque, and to follow the flat a priori *field below this altitude. In general, the true field is seen to be captured quite well where H_2O mixing ratios are <400ppmv, except at the edges of the cross-section.*

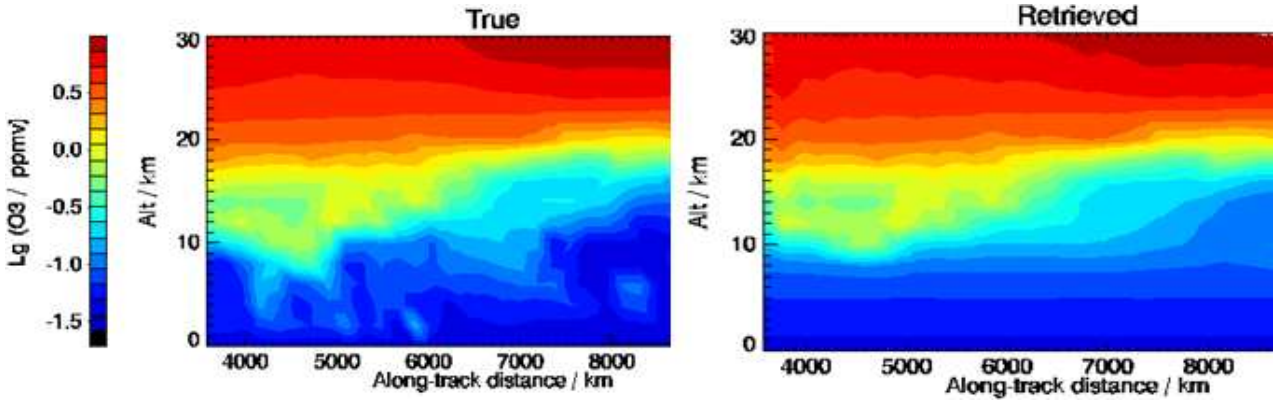

Figure 11: Iterative simulation of a 2-D O_3 cross-section retrieval from the MASTER 300 GHz band. Left and right panels are as in figure 10, except for O_3. The lower limit to which O_3 structure can be captured is determined by atmospheric limb opacity, which is governed by H_2O in this band, as it is in the 325GHz band and all other MASTER bands.

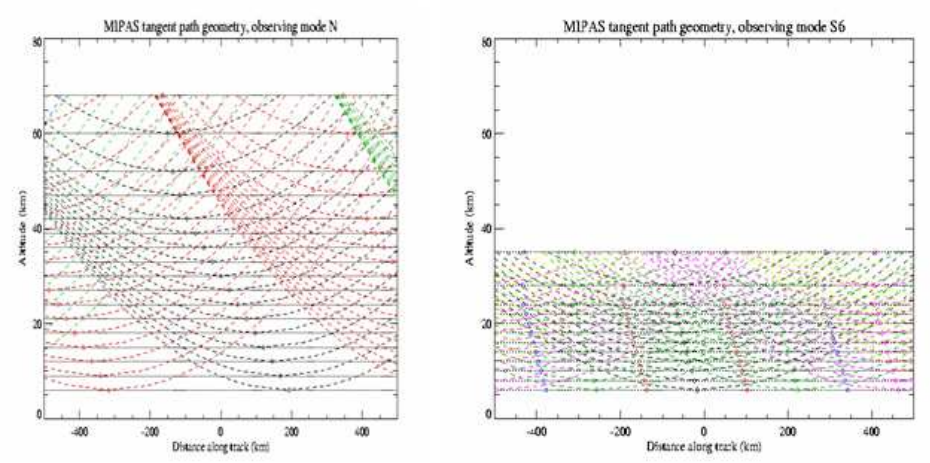

Figure 12: Limb-scan patterns for Envisat MIPAS normal mode and UTLS (S6) special mode. The left and right panels show tangent-paths for successive limb-views in the normal mode and S6 mode, respectively. In this projection, the Earth's surface is horizontal so the limb rays are curved. The much denser distribution of tangent-points in the S6 mode means that UTLS structure in the orbit plane is sampled sufficiently to exploit tomography, whereas in the normal mode it is not (see text).

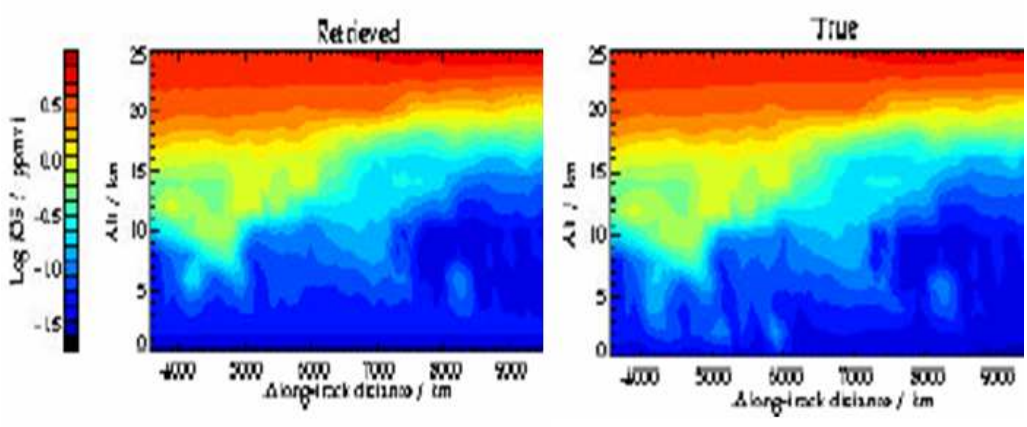

Figure 13: Iterative simulation of a 2-D O_3 cross-section retrieval from MIPAS in UTLS (S6) special mode (M.Parrington, pri.comm.). Left and right panels as for 11 except MIPAS. By comparison to 11, structure in the true O_3 field is seen to be captured down to lower altitudes (≈5km) by MIPAS than by MASTER. This is principally due to the selected IR window *extending to lower tangent-heights, but is also due to neglect of errors other than noise in the MIPAS simulation and to neglect of cloud.*

5 Summary and future work

A challenge for satellite remote-sensing is to measure the global distributions of important trace gases on the spatial scales required for research, monitoring and NWP. The viewing geometries and wavelengths of different techniques are complementary in terms of: detectable species, height range, vertical and horizontal sampling and resolution, penetration into the troposphere and susceptibility to cloud obscuration. The lower troposphere can be observed only with nadir geometry and ozone profiles spanning the troposphere and stratosphere can be retrieved by the RAL scheme from GOME observations. It is planned to process the full 8-year GOME mission with this scheme for evaluation by data assimilation models within DARC and ECMWF.

The vertical resolution is inherently higher for limb-emission geometry than for nadir geometry, permitting the stratosphere and upper troposphere to be observed with greater accuracy and hence the lower tropospheric information retrieved from co-located nadir observations to be maximized. Envisat offers the first opportunity to pioneer the technique of limb/nadir synergy together with tomographic limb-sounding. Limb/nadir synergy has been demonstrated in the retrieval domain by constraining a GOME Huggins'band retrieval with stratospheric O_3 produced operationally from Envisat MIPAS (ie L2 product). Simulations for mm-wave (MASTER) and IR (MIPAS) limb-sounders using the RAL tomographic scheme accurately capture 2-D structure in the UTLS and their intrinsic horizontal resolution has been shown to be much higher than that traditionally associated with limb-sounding. It is planned within DARC to pursue both these new techniques and to compare their implementations via retrieval and assimilation. A future mission to sound atmospheric composition from space should seek to exploit these new techniques as fully as possible.

Acknowledgements

Work presented in this paper was funded by NERC through the Data Assimilation Research Centre (DARC) and by ESA. The eigenanalysis of GOME averaging kernel matrices was provided by Vincent Soebijanta (BIRA-IASB) from work undertaken for ESA's GOME Ozone Profile Retrieval Working Group. The 2-D O_3 simulation for MIPAS was provided by Mark Parrington (D.Phil thesis, Dept of Physics, U.Oxford)

References

Fortuin, J. and Kelder, H. (1998). An ozone climatology based on ozonesonde and satellite measurements. *Journal of Geophysical Research - Atmospheres 103 (d24): 31709-31734*.

Kerridge, B., Reburn, W., Siddans, R., Smith, S., Watts, P., Remedios, J., Lama, F., Barnett, J., Murtagh, D., Stegman, J., Merino, F., Baron, P., Roscoe, H., Hausamann, D., Birk, M., Schreier, F., Schimpf, B., Lopez-Puertas, M., Flaud, J., von Clarmann, T., Stiller, G., Linden, A., Kellman, S., van Weele, M., Kelder, H., van Velthoven, P., Gauss, M., Isaksen, I., Hauglustaine, D., Clerbaux, C., and Boucher, O. (2001). Definition of Mission Objectives and Observational Requirements for an Atmospheric Chemistry Explorer Mission . *ESA Contract 13048/98/NL/GD, Final Report.*

Kerridge, B., Siddans, R., Latter, B., Burrows, J., Weber, M., Beek, R. D., Aben, I., and Hartman, W. (2002). GOME-2 Error Assessment Study. *Final Report EUMETSAT Contract No EUM/CO/01/901/DK.*

Langen, J. and Fuchs, J. (2001). ACECHEM - Atmospheric Composition Explorer for CHEMistry and climate interation. *ESA Report for Assessment SP-1257(4).*

Lary, D. (1995). Lagrangian four dimensional variational data assimilation of chemical species. *The Quarterly Journal of the Royal Meteorological Society , 121, 704.*

Siddans, R. (2003). Height-resolved ozone retrievals from gome. *PhD Thesis, University of Reading*.

Struthers, H., Brugge, R., Lahoz, W., O'Neill, A., and Swinbank, R. (2002). Assimilation of ozone profiles and total column measurements into a global general circulation model. *Journal of Geophysical Research-Atmospheres 107 (D20) art.4438*.